



UNIVERSIDADE ESTADUAL DE CAMPINAS SISTEMA DE BIBLIOTECAS DA UNICAMP REPOSITÓRIO DA PRODUÇÃO CIENTIFICA E INTELECTUAL DA UNICAMP

Versão do arquivo anexado / Version of attached file:

Versão do Editor / Published Version

Mais informações no site da editora / Further information on publisher's website:

https://www.osapublishing.org/oe/abstract.cfm?uri=oe-23-10-12582

DOI: 10.1364/OE.23.012582

Direitos autorais / Publisher's copyright statement:

©2015 by Optical Society of America. All rights reserved.

On-field distributed first-order PMD measurement based on pOTDR and optical pulse width sweep

Carolina Franciscangelis, 1* Claudio Floridia, 2 Glauco C. C. P. Simões, 2 Fernando Schmmidt² and Fabiano Fruett¹

¹University of Campinas, School of Electrical and Computer Engineering, Campinas, SP, 13083-970, Brazil CPqD, Campinas, SP, 13086-902, Brazil carolfra@dsif.fee.unicamp.br

Abstract: A method for PMD distributed localization and estimation based on polarization optical time domain reflectometer technique, pOTDR and pulse width sweep is used on-field for the first time. The method consists in launching light pulses with variable widths in an optical fiber under test and then analyzes the Rayleigh backscattered signal spatial power distribution after passing through a polarizer. Both localization and PMD magnitude are function of OTDR pulse width and can be obtained from the ripple analysis, enabling the characterization of the fiber links.

©2015 Optical Society of America

OCIS codes: (060.2370) Fiber optics sensors; (260.5430) Polarization; (260.2030) Dispersion; (060.2300) Fiber measurements; (290.5870) Scattering, Rayleigh; (120.4825) Optical time domain reflectometry.

References and links

- L. Carvalho, C. Floridia, C. Franciscangelis, V. Parahyba, E. P. da Silva, N. G. Gonzalez, and J. Oliveira, "WDM Transmission of 3x1.12-Tb/s PDM-16QAM Superchannels with 6.5-b/s/Hz in a 162.5-GHz Flexible-Grid using only Optical Spectral Shaping," Optical Fiber Communication Conference (OFC), M3C.3 (2014).
- R. Sabella, A. Bianchi, G. Bottari, F. Cavaliere, P. Iovanna, and F. Testa, "Trends in optical transport networks and related technologies," International Conference on Transparent Optical Networks (ICTON) (2014).
- N. S. Bergano, C. Poole, and R. E. Wagner, "Investigation of polarization dispersion in long lengths of singlemode fiber using multilongitudinal mode lasers," J. Lightwave Technol. 5(11), 1618-1622 (1987).
- G. J. Foschini and C. D. Poole, "Statistical theory of polarization dispersion in single mode fibers," J. Lightwave Technol. 9(11), 1439-1456 (1991).
- A. Galtarossa and C. R. Menyuk, Polarization Mode Dispersion (Springer, 2005).
- C. D. Poole, R. W. Tkach, A. R. Chraplyvy, and D. A. Fishman, "Fading in lightwave systems due to polarization-mode dispersion," Photonics Technology Letters, IEEE 3(1), 68–70 (1991).
- C. D. Poole and T. E. Darcie, "Distortion related to polarization-mode dispersion in analog lightwave systems," J. Lightwave Technol. 11(11), 1749-1759 (1993).
- F. Heismann, "Tutorial: Polarization mode dispersion: fundamentals and impact in optical communication systems," European Conference on Optical Communications (ECOC) 2, 51–79 (1998).
- N. Mantzoukis, C. S. Petrou, A. Vgenis, I. Roudas, and T. Kamalakis, "Performance comparison of electronic PMD equalizers for coherent PDM QPSK systems," J. Lightwave Technol. 29(11), 1721-1728 (2011).
- 10. B. Huttner, B. Gisin, and N. Gisin, "Distributed PMD measurement with a Polarization-OTDR in optical fibers," J. Lightwave Technol. **17**(10), 1843–1848 (1999).
- 11. R. Hui and M. O'Sullivan, Fiber Optic Measurement Techniques (Elsevier Academic Press, 2009).
- 12. C. Poole and D. L. Favin, "Polarization-mode dispersion measurements based on transmission spectra through a polarizer," J. Lightwave Technol. 12(6), 917–929 (1994).
- 13. G. C. C. P. Simões, C. Floridia, C. Franciscangelis, M. C. Argentato, and M. A. Romero, "Simultaneous nominal and effective differential group delay in-service monitoring method for optical communications systems," Opt. Express 21(7), 8190-8204 (2013).
- 14. A. J. Rogers, "Polarization-optical time domain reflectometry: a technique for the measurement of field
- distributions," Appl. Opt. **20**(6), 1060–1074 (1981).

 15. M. Wuilpart, G. Ravet, P. Megret, and M. Blondel, "Polarization mode dispersion mapping in optical fibers with a Polarization OTDR," IEEE Photon. Technol. Lett. 14(12), 1716-1718 (2002).
- 16. A. Ehrhardt, D. Fritzsche, M. Paul, L. Schuerer, D. Breuer, W. Weiershausen, N. Cyr, H. Chen, and G. W. Schinn, "Characterisation of the PMD distribution along optical fibres by a POTDR," 10th Anniversary International Conference on Transparent Optical Networks 1, 173–177 (2008).

- N. Cyr, H. Chen, and G. W. Schinn, "Random-scrambling tunable pOTDR for distributed measurement of cumulative PMD," J. Lightwave Technol. 27(18), 4164–4174 (2009).
- P. Fayolle, Y. Lumineau, G. Bouquet and V. Durel "Polarized lightwave reflectometry method (POTDR)," US7126678, filled: Oct., 10th, 2002. Concession Oct., 24th, 2006.
- C. Franciscangelis, C. Floridia, L. A. Ribeiro, and F. Fruett, "A Simple Method to Localize and Estimate PMD in Optical Fibers using the Polarization Optical Time Domain Reflectometry Technique," Latin America Optics and Photonics Conference (LAOP), LM3C.2 (2012).
- A. O. Dal Forno, A. Paradisi, R. Passy, and J. P. von der Weid, "Experimental and theorectical modeling of polarization-mode dispersion in single-mode fibers," IEEE Photon. Technol. Lett. 12(3), 296–298 (2000).

1. Introduction

Nowadays, fiber optics communications systems capacity experiences an ever growing evolution with the systems bit rate growing towards terabits per second [1, 2]. A fact that justifies such achievement is the use of optical fibers with low-power loss, low polarization mode dispersion, large effective area fiber (LEAF), among others. Polarization mode dispersion (PMD) is defined as a modal dispersion in which light travelling along a waveguide in two different polarization modes experiences a speed change between them [3–5]. This delay between both modes, generally around picoseconds, is caused by optical fiber birefringence, originated by waveguides intrinsic imperfections or external agents such as temperature, strain and stress [5].

High PMD in installed fibers is a bottleneck for the correct operation of an optical communication system, because it causes the broadening of the transmitted pulses, increasing the signal inter-symbol interference [6–8]. Thus, PMD degrades the transmitted signal quality and, therefore, limits the maximum data rate able to be transmitted and correctly received in any optical fiber network. Furthermore, the compensation of PMD in installed fibers is complex and expensive, generally employing an elevated number of taps for high PMD compensation, therefore it is reckoned as an undesirable method [9].

While the currently deployed optical fibers are rigorously specified for low values of PMD, the PMD value of the legacy fibers was not even measured before their installation. Thus, many legacy optical fiber networks exhibit high PMD sections that degrades transmitted data and, therefore, must be localized, measured and replaced [10]. Actually, there are plenty PMD measurement methods, but most of them are only capable to measure the PMD global value and they do not provide information concerning the PMD distribution along the analyzed fiber link [11–13]. The distributed measurement allows localizing the worst tracks in the fiber loop, that is, the sections with high PMD, enabling the network technician to easily replace them without the need to disconnect each track to measure its PMD. There are also some distributed PMD measurement proposals employing the polarization optical time domain reflectometer (pOTDR) technique. The technique is based on optical polarization and optical time domain reflectometer (pOTDR) [14–16]. However the pOTDR technique employments presented so far make use of transmitters and receivers of complex design or complex data processing methods [17]. Moreover, other similar proposals [18] use the value of ripple or related parameter P to obtain the value of PMD coefficient, cPMD, by an expression experimentally obtained. However, in [18] it is claimed that this method give good accuracy only over a range of 0.01 ps/km^{1/2} to 0.2 ps/km^{1/2}. This value corresponds to a maximum of 0.4 ps for a typical spun of 4 km. Thus, the method is limited to this amount of PMD, and also can only estimate the value of the PMD coefficient where ripple or relative noise is present.

In this work we validated on-field for the first time, a novel method based on the pOTDR technique, capable to localize high PMD sections in an optical fiber link and also estimate their DGD values. The proposed technique consists in launching light pulses with variable widths in an optical fiber under test and then, for each launched pulse width, analyzes the Rayleigh backscattered signal spatial power distribution after passing through a polarizer. The converted trace is the so called pOTDR curve and its behavior, when related to the launched OTDR optical pulse width, can provide information about the fiber PMD value distribution along the link length. We previously validated this technique, for the first time known, in

laboratory [19], estimating correctly the DGD of four different fiber sections in an optical fiber link.

This paper is structured as followed: Section 2 describes the proposed method; Section 3 reports a new laboratory validation of our method; Section 4 reports the on-field validation of the proposed technique, performed for the first time of our knowledge; lastly, Section 5 concludes the paper.

2. Description of the proposed pOTDR method

The proposed method operating principle is based on the analysis of the amplitude oscillations of pOTDR traces according the width variation of the optical pulses launched by an OTDR into the fiber under test. The experimental setup block diagram is presented in Fig. 1.

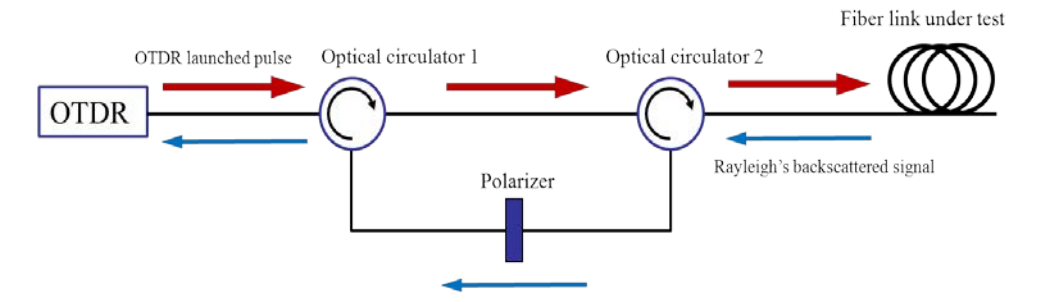


Fig. 1. Block diagram of the pOTDR method for distributed PMD measurement.

The OTDR launches optical pulses that are directed to the fiber link under test. The Rayleigh backscattered optical pulses that return from the optical link pass through the polarizer, responsible to convert SOP changes into optical power changes. This converted signal arrives at the OTDR, which exhibits the optical intensity *versus* distance curve for each width of the launched pulse.

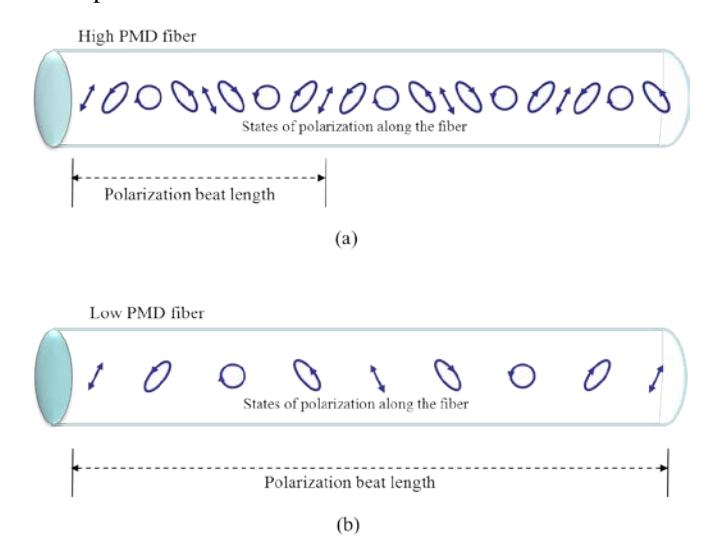


Fig. 2. State of polarization varying in (a) a high and (b) a low PMD optical fiber and its respective polarization beat length.

When a light pulse propagates through an optical fiber, its state of polarization will vary according to the fiber local birefringence. This phenomenon is characterized by the polarization beat length parameter, L_b , which is the necessary distance to be traveled by an

optical pulse in an optical fiber to repeat its initial state of polarization. The expression that relates first order PMD, meaning DGD, to L_b is:

$$\Delta \tau = \frac{\lambda L}{c L_b} \tag{1}$$

where $\Delta \tau$ is the fiber DGD, L is the fiber length, c the speed of light in vacuum and λ is its wavelength. It is noticeable from Eq. (1) that polarization beat length and DGD are inversely proportional unities, thus, fibers that exhibit high DGD values have lower polarization beat length than fibers with low DGD, as depicted in Fig. 2.

Therefore, a pulse launched by an OTDR that backpropagates through a high PMD fiber will experience more SOP changes per unit length than if it was traveling through a low PMD fiber. However, the SOP changes, converted into power oscillations by a polarizer as depicted in Fig. 1, will be detected at the OTDR reception unit, only if the space domain pulse width is of the same order of SOP variation in the fiber. It turn out, in practice, that at the OTDR screen, the pOTDR trace will be straighter in high PMD fibers than in low PMD fibers, where the trace will present ripples as depicted in Fig. 3.

The reason of this phenomenon is that SOP variations in optical fibers can only be detected by polarized light pulses whose space domain width is smaller than a quarter of the fiber polarization beat length value, and the SOP variations will be translate into high optical power amplitude fluctuations at the pOTDR curve. If pulse width is greater than $L_B/4$, the backscattered optical pulse SOP will be a sum of various SOPs, in other words, it will be depolarized and the SOP change will not be detected along this link, resulting in a small optical power fluctuation and thus in a straight line in the pOTDR curve. This fact makes feasible to qualitatively detected PMD impaired sections along a fiber link. This concept is resumed in Fig. 4.

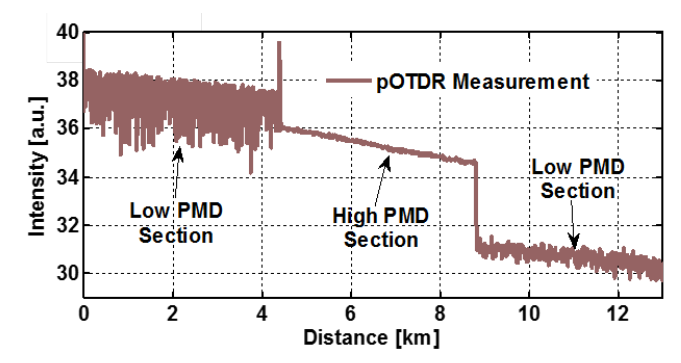


Fig. 3. Illustration of the pOTDR trace when a light pulse propagates through high and low PMD sections.

The main goal of the proposed method is to localize qualitatively the higher PMD sections. However, we also intended to estimate the DGD values of each fiber link section. In order to perform these estimations, we exploited another known property: the relation between DGD and OTDR pulse width. As previously explained, ripple appears when the OTDR pulse width in spatial domain, ζ , is equal or less than $L_B/4$, so, it ripples appears after launching a pulse of ζ width, than the maximum DGD presented in this fiber shall be:

$$\Delta \tau_{Maximum} = \frac{\lambda L}{cL_B} = \frac{\lambda L}{4c\zeta_{Ripple}} = \frac{\lambda L \Delta n}{2c^2 \Delta t_{FPWR}}$$
 (2)

where Δt_{FPWR} is the OTDR pulse width in time domain for which ripple is first observed, called in this work as the First Pulse With Ripple (FPWR). Therefore, in order to find the FPWR, one launches OTDR pulse from the largest to the shortest pulse width and analyses the ripple behavior. Furthermore, it is also possible to estimate a minimum DGD value, by

replacing Δt_{FPWR} in Eq. (2) by the previous OTDR available pulse width, called the Last Pulse Without Ripple, Δt_{LPWR} , which is larger than Δt_{FPWR} :

$$\Delta \tau_{Minimum} = \frac{\lambda L \Delta n}{2c^2 \Delta t_{LPWR}} \tag{3}$$

Therefore, one can estimate a DGD range for the L length fiber section as $\Delta \tau_{Minimum} \leq DGD \leq \Delta \tau_{Maximum}$. In order to classify a pulse as Δt_{FPWR} , Δt_{LPWR} or none, it was empirically obtained a ripple threshold. This value depends on the employed OTDR, so it is necessary to perform a calibration to obtain the threshold level.

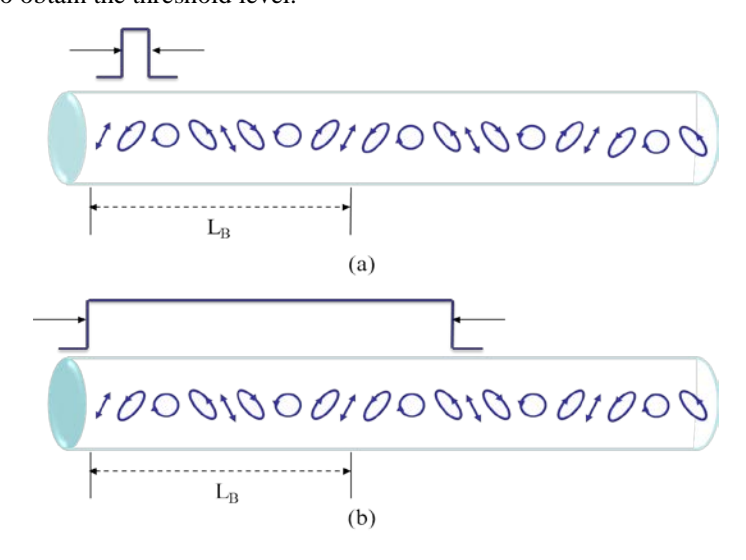


Fig. 4. Optical fiber traveled by (a) a polarized short width OTDR pulse and (b) a polarized large width OTDR pulse.

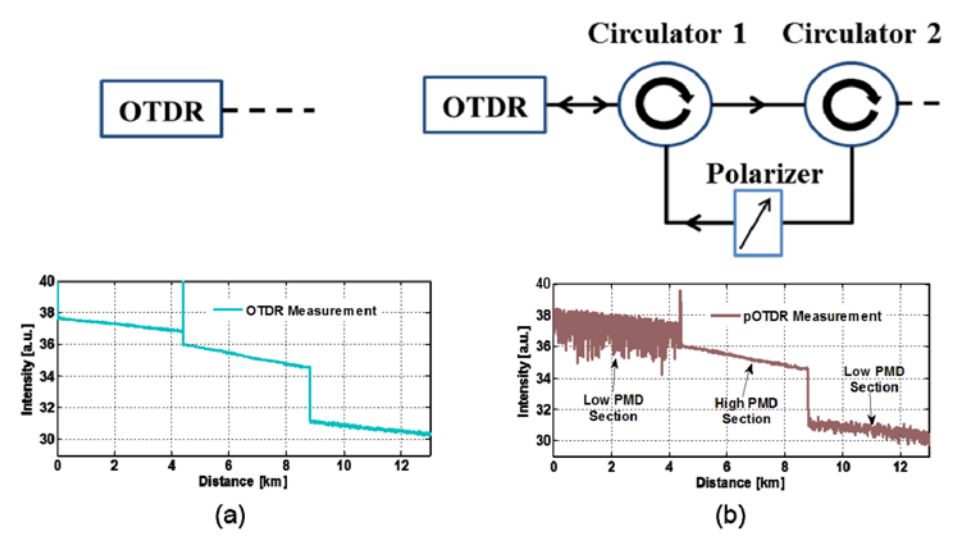


Fig. 5. Summary of the experimental setup configuration and characteristic traces for (a) OTDR mode and (b) pOTDR mode.

Thus, the pOTDR technique application can be explained and resumed as followed: i. Configure the system to operate as OTDR, according to Fig. 5(a). An optical 3 dB attenuator

is also used at the OTDR launch point to match the OTDR and pOTDR optical power levels; ii. Launch OTDR pulses from the largest to the shortest pulse width and acquire their respective OTDR curves. These OTDR traces will be used as reference to calculate the ripple curve; iii. Configure the system to operate as pOTDR, according to Fig. 5(b); iv. Launch OTDR pulses from the largest to the shortest pulse width and acquire their respective pOTDR curves; v. Subtract the pOTDR curve from the OTDR curve and extract its modulus for each pulse width. The modulus curves are the ripple *versus* distance traces; vi. Analyze the ripple traces of each fiber section and find their Δt_{FPWR} and Δt_{LPWR} with respect to the ripple threshold. Replace the Δt_{FPWR} and Δt_{LPWR} in Eq. (2) and Eq. (3), respectively in order to discover the DGD range for each fiber link section.

Figure 6 presents an example of OTDR, pOTDR and ripple curves obtained experimentally by applying our proposed method in a 4.4 km optical fiber section.

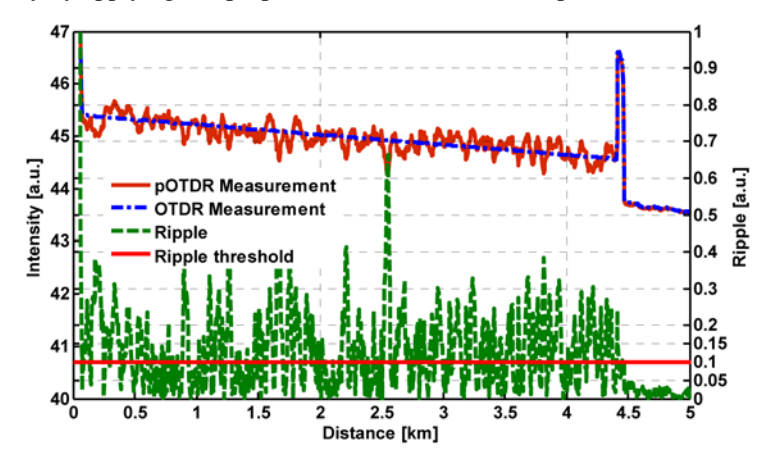


Fig. 6. Example of OTDR, pOTDR and ripple curves obtained experimentally with the proposed method.

The ripple threshold determination is defined as an OTDR previous calibration. This procedure is performed using an optical fiber whose DGD value is known. Each OTDR features limited options of available pulse widths. As previously explained, one can use Eq. (2) and Eq. 3 to traduce each pulse width to a superior or inferior correspondent DGD value limit. Thus, when calibrating an OTDR using a 0.8 ps/km fiber, it is verified that this DGD value that lies between 0.646 and 1.293 ps/km. Therefore, by Eq. (1) and Eq. 2, it is expected that the LPWR is 20 ns and the FPWR is 10 ns.

In order to estimate its OTDR ripple threshold, we analyze the 20 ns and 10 ns pulse width ripple traces. Considering the mean ripple for a pulse with 20 ns width as R_{LPWR} and the mean ripple for a pulse with 10 ns width as R_{FPWR} , then the ripple threshold is calculated as follow:

$$Ripple threshold = \frac{R_{LPWR} + R_{FPWR}}{2} \tag{4}$$

The ripple curve shown in Fig. 6 seems to be above the ripple threshold of 0.1 for a qualitative analysis. However, a more reliable quantitative analysis is necessary, so we also developed an auxiliary tool to analyze the ripple data, known as windowing. This technique consists of dividing the ripple curve of a fiber section into smaller subsections with predefined length. For instance, dividing a 5 km fiber section into 50 sub-sections of 100 m each, known as window size. Then, it is performed an average of all the ripple values present in each 100 m sub-section, obtaining a ripple curve with discrete values. This tool allows a better granularity in the DGD analysis.

The choice of the window size is arbitrary and depends only on the space resolution one needs to find the worst high PMD sections on a fiber link. Moreover, the window size choice

does not affect the accumulated DGD value estimation in a fiber section it only allows to localize the worst sub-sections inside this fiber section.

It is necessary to reinforce that our method does not measure the beat length. In fact the entire concept is based on the impossibility to measure the beat length which has its value less than the OTDR optical pulse width in the fiber, as in these cases the SOP variations cannot be detected. Thus, for issues regarding the decorrelation of fibers birefringence direction, it is expected that it does not affect significantly our method accuracy. In [20], Dal Forno et al demonstrated that the variation of number of concatenated elements and its length, despite the decorrelation, do not change the final PMD in more than 4% of its real expected value. Thus, this also corroborate for the validation of our method. Also in the case of high PMD section, a decorrelation means that SOP variation will be even faster and in this way a ripple-free trace will still arise. The minimum pulse width of pOTDR where this happens may vary and some PMD estimation error could occur, but the section will be correctly identified, and according to [20] we expect no significant deviations to occur. A better understanding of this issue is important but it is not the focus of this work. A simulation tool needs to be developed to study this behavior in further investigations.

In Section 3, we report a new laboratory validation of the proposed technique.

3. Laboratory experimental results

We performed a laboratory experiment similar to the one described in [19], but using three optical standard single mode fiber (SSMF) sections, each presenting different DGD values. Figure 7 illustrates the experimental setup, exhibiting each fiber length and reference DGD value, measured with a commercial OTDR, Anritsu CMA 5000A, and its wavelength is 1550 nm.

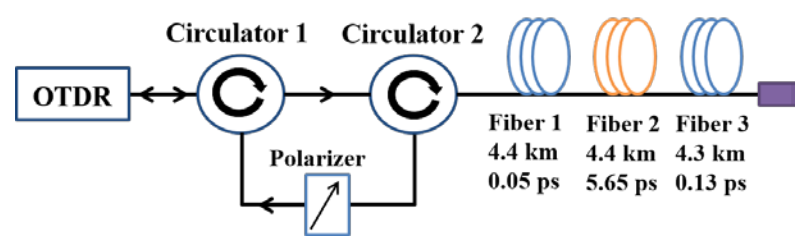


Fig. 7. Experimental setup illustration for laboratory validations.

The data acquisition followed the six steps iterative process resumed in Section 2, the same used in our previous laboratory validation with a four fibers link [19]. The OTDR, pOTDR and ripple curves acquired for each pulse width value are presented in Figs. 8, 9 and 10. It is relevant saying that the window size used in this data analysis was the length of each fiber section, 4.4 km, 4.4 km and 4.3 km, in order to estimate each fiber link DGD value.

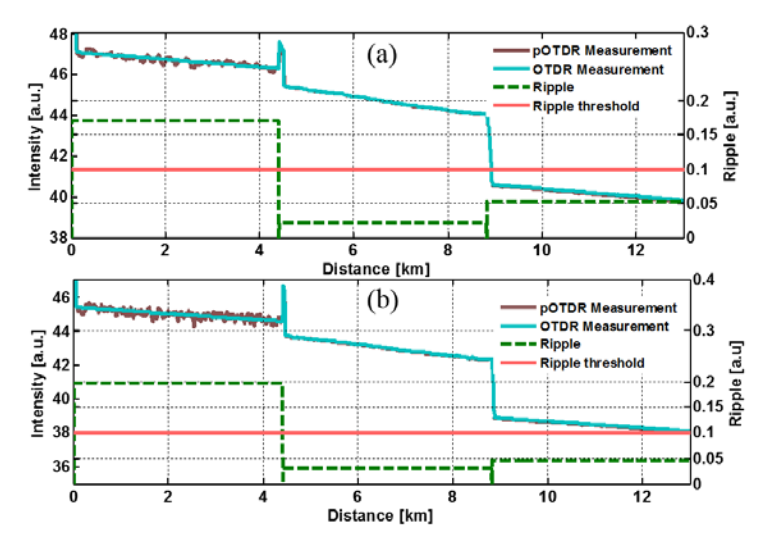


Fig. 8. Experimental laboratory results for (a) 1000 ns width pulses and (b) 500 ns width pulses.

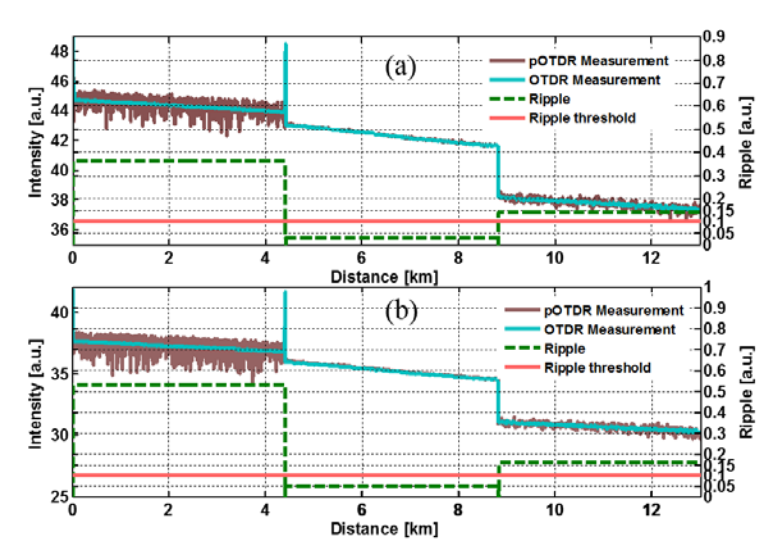


Fig. 9. Experimental laboratory results for (a) 100 ns width pulses and (b) 500 ns width pulses.

The data analysis of the curves presented Figs. 8, 9 and 10 is presented in Table 1, whose columns 2 and 3 show the values of the LPWR and the FPWR for each one of the three fiber sections. These obtained pulse widths values were inserted in Eqs. (2) and (3) to calculate inferior and superior DGD/km and DGD value limits, resumed in the columns 5 and 7. Finally, columns 4 and 6 show, respectively, the DGD/km and DGD reference values measured with commercial equipment.

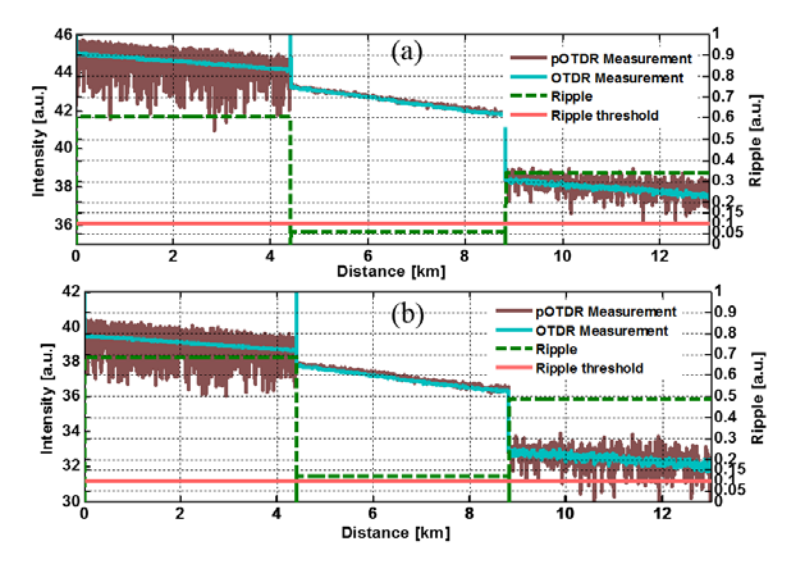


Fig. 10. Experimental laboratory results for (a) 20 ns width pulses and (b) 10 ns width pulses.

DGD/km DGD/km DGD DGD estimated measured estimated measured Fiber **LPWR FPWR** with with with with proposed commercial proposed commercial method section [ns] [ns] equipment method equipment [ps/km] [ps/km] [ps/km] [ps] LPWR > 1 100 0.011 < 0.013 0.050 < 0.057 100 from 0.646 to from 2.842 to 2 1.284 5.650 20 10 1.293 5.689 from 0.026 to from 0.112 to 3 500 100 0.030 0.130

Table 1. Results obtained from the data analysis of the laboratory experiments.

According to Table 1, we observe that all DGD values estimations performed with our proposed method are consistent with the measured DGD values using the commercial equipment. Both qualitative analysis and quantitative results testifies that the fiber section 2 beholds the highest DGD value when compared to the other two fiber tracks.

0.129

0.555

Moreover, we applied the square root of the sum of the squares on the three fibers reference measured DGDs and obtained a total maximum accumulated DGD of 5.65 ps. We performed the same calculus approach for the DGDs estimated with our technique and obtained 5.71 ps of total maximum accumulated DGD, which represents a relative error of 1.1% when compared to the calculated 5.65 ps reference. Thus, we validated once more our method in laboratory environment, which reinforces its repeatability capacity.

In Section 4, we report an on-field validation of our technique.

4. On-field experimental results

In this section we describe an on-field application of our proposed method to measure distributed PMD along fiber links. This measurement was performed on a real optical fiber network link with a total length of 19.75 km. For these experiments, an EXFO FTB-730 commercial OTDR was used. However, it was not possible to proceed to this OTDR threshold calibration before on-field tests. Therefore, for field data we opted to change the ripple threshold in that way that accumulated PMD, calculated via square root of sum of squares, approximate the overall know value, in a sort of post-calibration. Thus, the post-calibrated ripple threshold value is 30 mdB. The OTDR pulse width was varied from 50 ns to 5 ns. In

order to facilitate the traces analysis, we divided the curves in six sections and named them according to Fig. 11.

We also measured the accumulated PMD of the whole A-F fiber link using commercial equipment, EXFO FTB-5500B, which measured 29 ps.

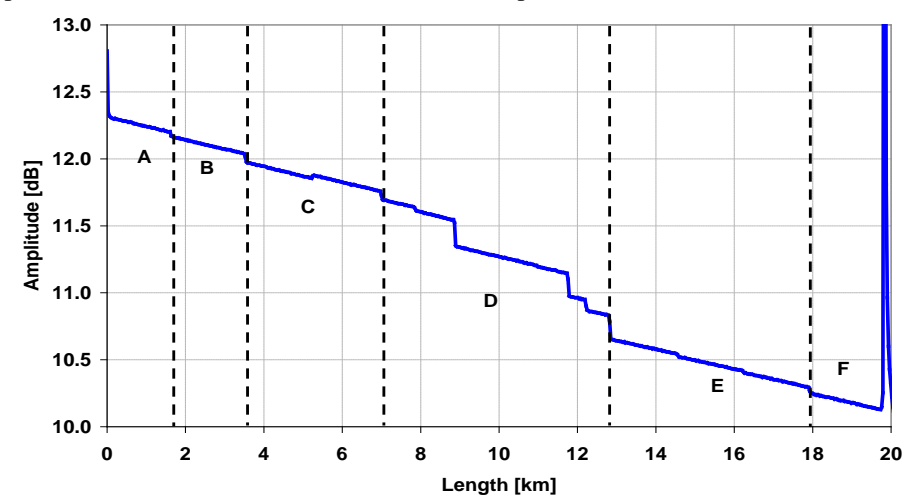


Fig. 11. OTDR curve with the identification of the six divided fiber sections.

We performed the data acquisition according to the six steps iterative process presented in Section 2, the same used in our laboratory validations. In these on-field experiments, though, we employed a windowing of 500 m in the ripple curves. It means that we divided our six fiber sections into sub-sections of 500 m and averaged each one of them. Thus, we were able to analyze this fiber link PMD behavior with a resolution of 500 m.

The OTDR, pOTDR and ripple curves acquired for each pulse width value are presented in Figs. 12 and 13.

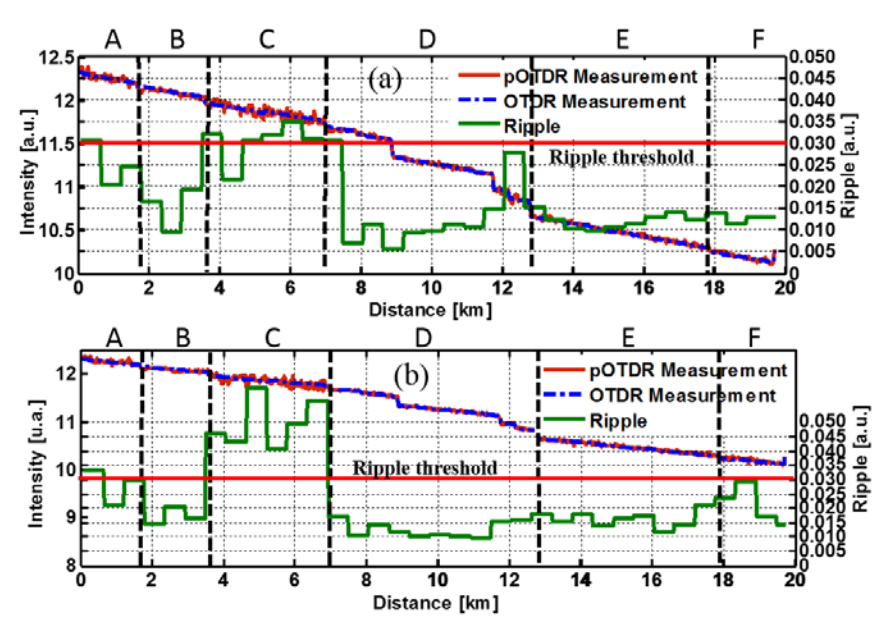


Fig. 12. Field trial results for (a) 50 ns width pulses and (b) 20 ns width pulses.

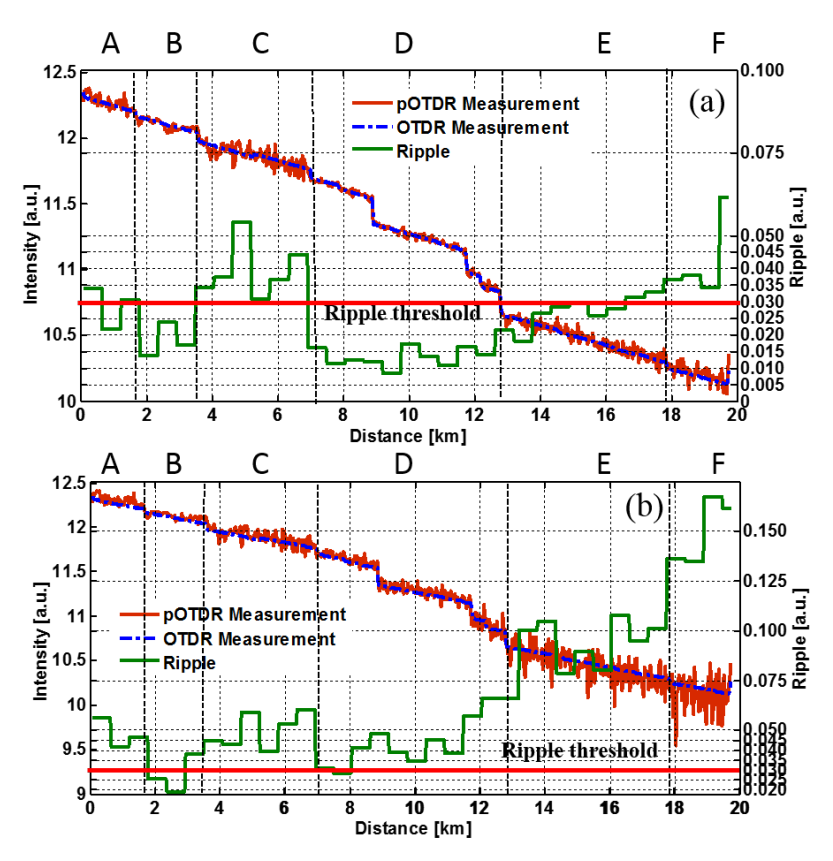


Fig. 13. Field trial results for (a) 10 ns width pulses and (b) 5 ns width pulses.

The visual inspection of the ripple traces presented in Figs. 12 and 13 leads to conclude that the sections B and D are the fiber sections that contribute the most for the link high PMD value. It is inferred due to the fact that their ripple are lower than the other sections ripple, and section B FPWR measurement was not even possible to measure with the current OTDR whose minimum pulse width is 5 ns. Thus, according to our analysis, fibers B and D strongly contribute to the 29 ps global PMD of the fiber link, measured with commercial equipment.

We evaluated the DGD values range of the six fiber sections from A to F according to the step number 6 of the procedure presented in Section 2. Table 2 summarizes the quantitative DGD values estimated.

Fiber section	Length [km]	DGD estimated with proposed method [ps]	FPWR [ns]	LPWR [ns]
A	1.65	2.13 < DGD < 4.27	5	10
В	1.88	4.87 < DGD	FPWR < 5	5
С	3.45	0.45 < DGD < 0.89	50	100
D	5.85	7.55 < DGD < 15.15	5	10
E	5.15	6.64 < DGD < 13.33	5	10

1.15 < DGD < 2.28

Table 2. Quantitative results obtained in the field trial data analysis.

It is noteworthy to observe that a visual inspection of Fig. 13(a) will show that fiber section E ripple seems to reach the threshold before fiber section D. However, as our OTDR didn't presents an optical pulse width between 5 and 10 ns, we weren't able to estimate section E FPWR with more accuracy.

10

20

F

1.77

We calculated the maximum accumulated DGD for each fiber section and also for the whole 19.75 km link by using the square root of squares sum equation:

$$\Delta \tau_{Accumulated} = \sqrt{DGDMax_A^2 + DGDMax_B^2 + ... + DGDMax_F^2}$$
 (5)

According to the maximum estimated DGD values of each fiber section, the square root of squares sum result for maximum accumulated DGD is 21.34 ps, which presents a 36% relative error when compared to the 29 ps measured with commercial equipment. However, an important detail must be considered: we could not measure the FPWR for the fiber section B using an OTDR with minimum pulse width of 5 ns. Observing the ripple trace for 5 ns on section B, we concluded that it was far from reaching the ripple threshold. Thus, we simulated a new DGD analysis for fiber section B, considering its FPWR as 1.25 ns. This simulated FPWR leaded to a maximum fiber section B DGD of 19.44 ps and a total accumulated DGD of 28.45 ps. This new value represents a 1.9% of relative error, when compared to the 29 ps of accumulated DGD measured with commercial equipment. Also, it must be considered the granularity of the method that provides intervals of PMD estimated values of PMD instead of an exact value due to the OTDR available optical pulse widths.

Figure 14 depicts the maximum accumulated DGD evolution along the on-field fiber link for both approaches: with (blue full line) and without (red dashed line) the use of 1.25 ns pulse width.

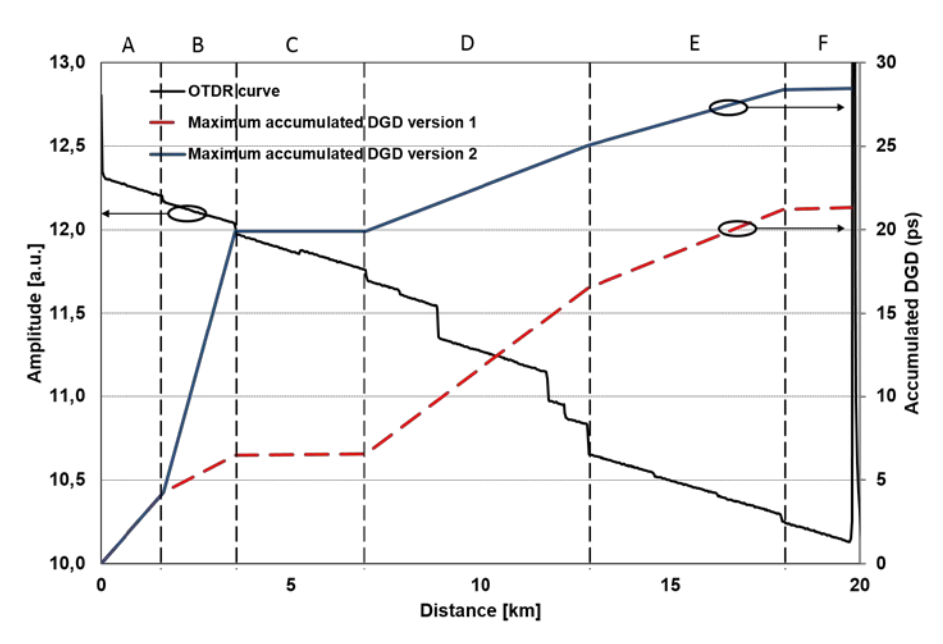


Fig. 14. Estimated accumulated DGD evolution along the on-field fiber link for approaches with (full blue line) and without (dashed red line) the use of a 1.25 ns pulse width.

Moreover, the information obtained by our proposed technique makes possible corrective actions by the optical fiber field technicians. In this case, if one replaces both the fiber sections B and D by a fiber of low DGD, 0 ps assumed for simplification, it would be sufficient to reduce the total accumulated DGD to 14.21 ps. Furthermore, if we could also replace section E, which also presents a high PMD, the total accumulated DGD would drop to 4.93 ps. This reduction couldn't be validated experimentally, because it wasn't possible to unbury each fiber section to measure its individual DGD and replace the worst one. Nevertheless, this simulation may be a feasible tool for a technician to analyze the impacts of changing each fiber section before performing the replacement.

5. Conclusion

We validated a method to measure distributed DGD along a fiber link both on laboratory and on-field. In order to achieve this goal, we proposed a distributed DGD measurement technique based on polarization optical time domain reflectometer, pOTDR and on OTDR pulse width sweep.

We previously validated the proposed method by performing laboratory tests, whose estimated DGD values results were coherent with those measured with commercial equipment used as reference. In this work, we validated this proposal on another laboratory setup configuration, testifying the repeatability of our method. Then, we performed an on-field experiment in order to testify its reliability on real optical networks. The results shown that the technique was able to localize high PMD fiber sections in a 19.75 km length link on-field. Moreover, we claimed and justified that if we could use an OTDR with shorter pulse widths, we would be able to estimate a total accumulated DGD value of 28.45 ps, which represents a 1.9% of relative error when compared to the result of 29 ps measured with a commercial equipment. It is important to emphasize that the proposed method provides an estimative of PMD and that there is a trade-off between reach and resolution of an OTDR. Shorter pulses may provide us better accuracy, but at the expense of shorter reach, which stands as the main limitation of our developed method and is an issue to be investigated and improved in further researches.

The proposed method presented acceptable accuracy when applied to measure PMD in currently deployed fibers, as demonstrated in both laboratory and on-field experiments. Thus, this is further evidence that the variations in the decorrelation length of these fibers birefringence axes do not affect significantly the total amount of PMD, as stated in literaturare. Simulation tool also needs to be developed as a future work to better study and model this decorrelation effect, even if literature reports only 4% impact on the PMD in such cases.

Also, we performed a simulation demonstrating the total accumulated DGD estimated value drop to 4.93 ps when replacing the highest PMD sections, B, D and E, for 0 ps DGD fiber tracks. Therefore, we evaluated the application of the proposed technique on field deployed fibers, where this method proved to be a useful tool for optical network technicians despite its current limitations.

Acknowledgments

The authors would like to thank the Brazilian Federal Agency for the Support and Evaluation of Graduate Education - CAPES - for their financial support in order to cover the expenses to publish this article. CNPq sponsors C. Floridia under scholarship DT.